VACUUM ULTRAVIOLET RADIATION EMITTED FROM ARC-JET PLASMAS OF ARGON OR NITROGEN

G. E. Staats and W. K. McGregor, Jr.
ARO, Inc.
and
A. A. Mason
The University of Tennessee Space Institute

October 1968

ROCKET TEST FACILITY
ARNOLD ENGINEERING DEVELOPMENT CENTER
AIR FORCE SYSTEMS COMMAND
ARNOLD AIR FORCE STATION, TENNESSEE

NOTICES

When U. S. Government drawings specifications, or other data are used for any purpose other than a definitely related Government procurement operation, the Government thereby incurs no responsibility nor any obligation whatsoever, and the fact that the Government may have formulated, furnished, or in any way supplied the said drawings, specifications, or other data, is not to be regarded by implication or otherwise, or in any manner licensing the holder or any other person or corporation, or conveying any rights or permission to manufacture, use, or sell any patented invention that may in any way be related thereto.

Qualified users may obtain copies of this report from the Defense Documentation Center.

References to named commercial products in this report are not to be considered in any sense as an endorsement of the product by the United States Air Force or the Government.

VACUUM ULTRAVIOLET RADIATION EMITTED FROM ARC-JET PLASMAS OF ARGON OR NITROGEN

G. E. Staats and W. K. McGregor, Jr.
ARO, Inc.
and
A. A. Mason
The University of Tennessee Space Institute

AF - AEDC
Arnold AFS Tenn

FOREWORD

The work reported herein was sponsored by the Arnold Engineering Development Center (AEDC), Air Force Systems Command (AFSC), Arnold Air Force Station, Tennessee, under Program Element 61102F, Project 8951, Task 895105.

The results of research presented were obtained by ARO, Inc. (a subsidiary of Sverdrup & Parcel and Associates, Inc.), contract operator of the AEDC, under Contract F40600-69-C-0001. The research was conducted from August 1, 1967 to August 1, 1968 under ARO Project Nos. RW5709 and RW5805 and ARO subcontract to UTSI 68-27-TS/OMD in the Propulsion Research Area of the Rocket Test Facility (RTF), and the manuscript was submitted for publication on July 9, 1968.

The authors wish to acknowledge the assistance of Mr. Charles E. Redman, RTF, ARO, Inc., who had a great part in the fabrication of most of the apparatus.

This technical report has been reviewed and is approved.

Terry L. Hershey
Captain, USAF
Research Division
Directorate of Plans
and Technology

Edward R. Feicht
Colonel, USAF
Director of Plans
and Technology

ABSTRACT

Vacuum ultraviolet emission in the range from 2000 to 700 Å was observed for both argon and nitrogen plasmas, produced by a Gerdien-type arc-jet freely expanding into a vacuum cell. The experimental setup centers about a simple, one-meter, concave grating spectrograph mounted within a tank purged with helium. Other gases were allowed to mix with the flowing plasma so that the physical mechanisms of excitation within the plasma could be studied. Over 50 atomic lines and three band systems were identified in mapping the spectral region. Mechanisms to produce the radiation observed are postulated, and some unexplained phenomena are also discussed.

CONTENTS

APPENDIXES

I. ILLUSTRATIONS

Figure

SECTION I
INTRODUCTION

An experimental investigation was undertaken to determine the feasibility of obtaining vacuum ultraviolet spectral data from an arc-jet plasma. The vacuum ultraviolet (VUV) is that portion of the electromagnetic spectrum extending from 2000 to 10 Å; however, this effort was restricted to the range from 2000 to 700 Å. Although the spectroscopy of high-enthalpy gas flows is not new, this is believed to be the first VUV study of this type of plasma.

This report describes the exploratory phase of a continuing investigation in the VUV spectral region which, together with research in other spectral regions, has as its goal the understanding of the collisional and radiative processes within the plasma. The initial tasks reported on here are the development of VUV observational methods in a test cell environment, the mapping of the VUV spectral region, and a determination of the excitation energies involved in the radiation emission.

When the investigation was initiated, it was not known to what extent short wavelength radiation was emitted by the plasma or if such radiation could be observed in the test cell environment. The primary effort was directed toward the development of observational techniques in the wavelength region below 2000 Å where difficulties arise because constituents of the air absorb strongly in this region. The simplest and quickest approach was to adapt a one-meter Cenco® spectrograph to the VUV region by replacing the original diffraction grating with a spherical, 1200-line-per-mm reflection grating blazed for 1500 Å and to purge the optical path inside the instrument with helium or argon. This avoided the purchase of specialized instrumentation and the expense of a complicated system of differential pumping required to maintain a high vacuum in the presence of a flowing plasma.

Over 50 lines and three band systems involving 40 bands were identified in mapping the spectral region, and their frequencies were determined. Although emission from atomic and molecular species was observed, there was no ionic or continuum radiation recorded. Emitting species were combinations of argon, nitrogen, oxygen, hydrogen, carbon, and carbon monoxide, depending on the operating circumstances.

Several theoretical models have been proposed for describing the microscopic energy transfer mechanism in the field-free plasmas produced by expanding the hot gas from an arc-jet into a vacuum cell maintained at about 1 torr. Brewer and McGregor (Ref. 1) proposed that the

visible plume radiation extending far downstream was due to the existence of relatively high densities of argon atoms in metastable states. This enhanced the probability of collisional excitation to upper excited states, which then decayed to lower energy levels with the emission of radiation. Robben, Kunkel, and Talbot (Ref. 2) used the collisional-radiative-recombination model to explain their results from a similar He plasma. Bowen (Ref. 3) pointed out that the result would be the same if the over-populated states were the resonance states which could be excited by absorption of the resonance lines produced in the arc. Such models provide an understanding of physical processes which is fundamental to the correct interpretation of the spectral radiation from such plasmas. The present investigation resulted from the need to assess the relative importance of resonance absorption and metastable atom collisions in the excitation processes of argon. In argon, transition from both the resonance and metastable levels to the ground state gives rise to atomic line radiation of wavelengths around 1050 Å. Hence, studies in the VUV might lead to a direct measure of excitation energies and produce insight into the excitational mechanism.

SECTION II
APPARATUS

2.1 ARC-JET AND TEST CELL

A diagram of the arc-jet and test cell is shown in Fig. 1 (Appendix I). The d-c arc-jet is of the conventional Gerdien design with a tungsten cathode and copper orifice anode (Ref. 4). The working gas enters the arc chamber from the rear, flows at about 1 $g\text{-}sec^{-1}$ through the arc region, and exits through a 0.64-cm orifice into the test cell. As the gas passes through the arc region, 6 to 7 kw are transferred to the gas by collisions with the electrons in the arc. The free jet flows from a pressure of 300 to 800 torr in the arc chamber into the 15.24-cm-diam vertical, stainless steel test cell, which is evacuated by two large mechanical vacuum pumps to about 1 or 2 torr. The visible radiating free jet expands to a diameter of 8 to 10 cm and extends about 1 m beyond the orifice. Concentric with the free jet and in the plane of the exit orifice is a ring of tubing, drilled with small holes, through which different gases were introduced into the periphery of the free-jet plume. The test cell has one small viewing port and a port to which the spectrograph is attached. The arc-jet is secured to the bottom of the test cell and sealed by an O-ring on the head of the arc-jet.

The 15.24-cm-diam cross section for the test cell was chosen with two competing factors in mind. It was desired (1) to study a freely

expanding plasma with no impingement on the walls of the test cell, and (2) to keep gaseous impurities (gases other than the working gas) to a minimum. This was accomplished by making both the volume and the interior wall surfaces of the test cell as small as possible. Thus, the volume of ambient gas and the amount of outgassing from the wall were minimized.

2.2 SPECTROGRAPH

A Cenco grating spectrograph, designed for use in the 3000 to 7000 Å wavelength region, was used. The original grating was replaced with a new 1200-lines/mm concave reflection grating having a 1-m radius of curvature, a coating of MgF_2, and a blaze angle for 1500 Å. This grating was mounted in the original grating holder and rotated about a vertical axis to display the spectral region from central image to 2000 Å on the film pack. Preliminary experiments indicated that radiation was being emitted in this spectral region and meaningful data could be obtained. However, the instrument was inadequate because the entrance slit could not be focused across the entire exit plane where the film was placed. The decision was made to realign the optical path, maintaining the Paschen-Runge mount of the concave reflection grating (Fig. 2). This mounting provides an optical path with a single reflection, which is a distinct advantage in the VUV region where reflection losses become prohibitive (Ref. 5). Realignment was accomplished by disassembling the instrument, mounting the film pack-slit assembly on an aluminum sheet, and repositioning the grating holder unit with respect to the assembly on the same aluminum sheet. This arrangement of the components provided a sharp focus over the complete 2000-Å range displayed on the film. Final focus produced a resolution of approximately 0.5 Å at 1500 Å and a reciprocal linear dispersion of about 8.2 Å/mm.

The film pack was modified to accommodate 35-mm, Kodak SWR film. The film was inserted into a specially constructed, curved, stainless steel film holder and then placed in the original Cenco film pack. Felt was placed around the edges of the film holder to form a light-tight seal.

The instrument is contained in a 75-cm-diam tank flanged to a port on the test cell (Fig. 1). The spectrograph viewed the plasma plume 10 cm downstream of the exit orifice, with the slit parallel to and aligned along the plume axis. Because atmospheric gases strongly absorb radiation below 2000 Å, it was necessary to eliminate or reduce the air in the optical path. This can be done by high vacuum techniques

or by replacing the air with a nonabsorbing gas. In these experiments, the tank was continuously purged with helium or argon at a pressure slightly greater than the test cell pressure during film exposures. By this means the need for maintaining a high vacuum in the spectrograph by differential pumping was eliminated. Between runs, the spectrograph tank was normally maintained at a pressure of less than 10^{-3} torr to prevent surface adsorption of unwanted gases.

For localized studies, a viewing tube (Fig. 3) was inserted into the port through which the spectrograph views the plasma. The stainless steel tube with an end plate extended into the plasma and restricted the viewing of the VUV radiation to the spatial region of interest. The flattened tube was aligned parallel to the slit and the plasma flow.

SECTION III
EXPERIMENTAL TECHNIQUES

3.1 OPERATING AND SPECTROGRAPHIC TECHNIQUES

The operational procedure was based on an effective purging technique developed during the course of this investigation. At the beginning of each run, the loaded film pack had to be placed in the spectrograph. This was accomplished by bringing the normally evacuated spectrograph tank up to atmospheric pressure by the inflow of helium or argon and inserting the film pack into its holder through a port in the side of the tank. The tank was then pumped down and purged by establishing a small flow of helium into the spectrograph tank. The arc-jet was started and operated with either argon or nitrogen as a working gas as described by Dooley, McGregor, and Brewer (Ref. 4). After a run, the tank was bled back up to atmospheric pressure with helium, the film pack was removed, and the tank was reevacuated.

The film pack was positioned vertically through a 5-cm range by a racking mechamisn operating from outside the tank. A mask in front of the exit plane limited the image to 0.55 cm in height, and this, together with the vertical movement, allowed five exposures on a single film strip. A manually operated valve isolated the spectrograph tank from the test cell and acted as the shutter for the instrument.

Exposure times ranged from 5 sec to 20 min, depending on the experiment, but most data were taken using 10-min exposures. Often one exposure was stopped and the next started simply by racking the film pack into the next position. The spectral region lying between the

central image and 2000 Å was displayed on the film. Because of limitations inherent in this near-normal incident instrument, wavelength cutoff was estimated to be about 600 Å, but only spectra between 790 and 2000 Å were actually observed.

In these preliminary studies, the primary concern was not with restricting the field of view to a limited region of the plasma but with obtaining sufficient intensity of radiation to ensure that no important spectral characteristics were unobserved. Consequently, the field of view (Fig. 4) was determined by the spectrometer slit as an objective stop and the 2.54-cm-diam entrance port to the test cell as a field stop. These two stops were spaced 30.5 cm apart. This arrangement provided adequate energy but resulted in viewing an elliptical cone through the plasma which had about a 5- by 4-cm cross section at the centerline of the plume.

3.2 PHOTOGRAPHIC TECHNIQUES

The darkroom in the RTF Research Optical Laboratory was equipped for processing Kodak SWR film. The simple five-step procedure, which is fully described in the handbook, Kodak Plates and Films for Science and Industry, gave satisfactory results. The film was

1. Soaked for 2 min in distilled water (68 to 70°F),
2. Developed for 2 min in a developing solution of 1:1 Kodak D-19 and distilled water (68 to 70°F).
3. Stopped for 30 sec in Kodak indicator stop (68 to 70°F) (initially, water was used as a stop),
4. Agitated for 4 min in Kodak rapid fixed (68 to 70°F), and
5. Washed 20 min in running tap water (68 to 70°F).

Typical film strips are shown in Fig. 5. To date, film with a perfectly clean background has not been obtained. Small specks appear at random over the film strip. These are bothersome only when viewing the film strip with a microdensitometer. They produce spurious data in the form of line-like profiles on the chart paper which must be noted by an observer to prevent erroneous interpretations of the data. Considerable effort has been made to eliminate this problem. The number and size of the spots have been reduced from the original film strips by taking the utmost care with purity of the chemicals and cleanliness of the darkroom apparatus. Varying the time between the removal of the film from the

storage freezer and the exposure of the film had little effect on the clearness of the film background. Finally, however, constant agitation of the film in the fixer appeared to be the most effective means of reducing the spotty background. It is felt that the appearance of the film strips can be improved even more, and experiments with data-taking methods and dark room techniques are continuing.

3.3 DATA REDUCTION TECHNIQUES

In these studies, data reduction consisted of determining the frequency location of the observed spectral lines and bands and the identification of the emitting species. There was no continuum present, and no intensity measurements have been made at this time. A distinct advantage of the VUV spectral region is the simplicity of the spectra of monatomic gases, consisting of the atomic resonance radiation and the many-line convergence to the ionization potential. Observations in other spectral regions of similar argon arc-jets by Brewer and McGregor (Ref. 6) suggested that only atomic argon line radiation and molecular nitrogen band radiation would normally appear in the VUV. Instead, the spectrum consisted of the expected argon lines and many unexpected atomic lines at longer wavelengths, as shown in Fig. 5. The identification of these lines then became a major part of this work.

The lines were identified in the following manner. A small amount of hydrogen was allowed to mix with the flowing argon plasma. The many-lined spectrum of the hydrogen molecule was excited, plus six lines of the Lyman series of atomic hydrogen. The H_α line (1215.7 Å) of the Lyman series was considerably enhanced and was also one of the lines that always appeared on the filmstrip. The ratio of the wavelength of H_α to the distance in millimeters between H_α and the central image gave a reciprocal linear dispersion of 8.2 Å/mm. This dispersion was used to obtain approximate wavelengths for the more prominent lines on the filmstrip. Comparison of these approximate wavelengths with a table of wavelengths (Ref. 7) provided tentative identification of about 20 lines of atomic argon, oxygen, nitrogen, and hydrogen. It was apparent, however, that the dispersion was varying with wavelength, and if the remaining lines were to be identified (and the tentative lines verified), an accurate dispersion curve would be required.

The relative positions of the lines on the filmstrip were transferred to chart paper by means of a recording densitometer. The line centers were determined, and their distance from central image on the chart paper was measured. By using the accurate wavelengths of the identified lines of atomic argon, hydrogen, oxygen, and nitrogen, the linear dispersion was calculated at various points throughout the spectral

range. The calculated dispersions were plotted as a function of distance from central image for the spectral range from 1000 to 2000 Å. Positive identification of additional lines permitted slight corrections to the dispersion curve and its extension into the shorter wavelength region. This curve (Fig. 6) allowed the determination of the vacuum wavelength at any position on the chart paper to within a few tenths of an angstrom and resulted in the identification of over 50 lines and bandheads (Table I, Appendix II).

Since one of the purposes of these studies was to determine the energy levels excited in this type of plasma, the final step in the identification program was to determine the transition, that is, the initial and final energy levels of each spectral line observed. Dr. R. L. Kelley's report (Ref. 8) provided the necessary information. The results of the transition determinations are also listed in Table I and shown schematically in Figs. 7 through 11.

Three or four groups of lines, not completely resolved, were attributed to carbon. It was possible to resolve lines separated by as little as 0.6 Å, but this was apparently not sufficient to resolve these carbon lines.

In addition to the atomic spectral lines, molecular bands made their appearance under certain operating conditions. The most pronounced of these bands were the N_2 Lyman-Birge-Hopfield bands, which appeared when N_2 was added, and the fourth positive band system of CO, which appeared with the addition of CO_2 around the argon plume. Some 20 bandheads of the CO band system were observed and identified, as were 18 of the N_2 Lyman-Birge-Hopfield system. In both, identification was facilitated by displaying the bandheads in a Deslandres table, as shown in Tables II and III.

SECTION IV
EXPERIMENTS PERFORMED

4.1 ARGON PLASMA

Initially, the arc-jet was operated with argon as the working gas and with no foreign gases added into the test cell except for the small inflow of helium from the spectrograph. The arc-jet plume was light red to pink in color. The radiation consisted of 21 atomic argon lines and approximately 20 additional lines of contaminant gases (Table IV). The two resonance lines of argon at 1048 and 1066 Å were observed

together with 19 argon lines resulting from electronic transitions from higher excited states directly to the ground state (Figs. 7 and 8). However, of the 19 lines, five could be unresolved doublets, and thus possibly 24 of these higher transitions could be occurring. The contaminants appeared to be ambient gases in the test cell, and considerable effort to eliminate them was only partially successful. The relative intensities of lines emitted by contaminant gases varied slightly from run to run; however, some line radiation from nitrogen, hydrogen, crabon, and oxygen was always observed in the argon jet. The lines normally observed are identified in Table IV.

4.2 NITROGEN PLASMA

Only a few filmstrips were taken of the arc-jet operating with nitrogen. The visible nitrogen plume was a lighter pink than the argon and smaller in diameter. Either helium or argon was used as the purge gas in the spectrograph when nitrogen was the working gas.

Only atomic line radiation was observed in the nitrogen plasma. Although nitrogen band radiation might be expected, none was observed; and since the nitrogen plasma observations were a minor part of this study, the matter was not pursued at this time. The contaminants radiating in the VUV were hydrogen, oxygen, and carbon which. with the exception of nitrogen, were the same as those observed in the argon jet. Nitrogen may have been a contaminant also, but since it was the working gas, there was no way to determine this. The intensity of the oxygen triplet (1302, 1304, and 1306 Å) in the nitrogen arc-jet was much reduced over that in the argon arc-jet for corresponding exposure times but still appeared.

It should be noted that only two groups of observed N lines, the 1200- and 1134-Å groups, were the result of direct transitions to the ground state. The lower states of the remaining transitions were evenly divided between the two metastable levels at 2.38 and 3.58 ev (Fig. 9). The lines observed in the nitrogen plasma are listed in Table V.

4.3 ARGON PLASMA WITH MIXING OF VARIOUS GASES

The arc-jet was operated with argon as the working gas. Around the exit orifice of the arc-jet, a ring of tubing drilled with many small holes allowed the mixing of various gases into the periphery of the plasma flow. The radiation emitted by the various gases was measured

to provide some insight into the excitation mechanisms and the energy properties of the flowing plasma.

4.3.1 Hydrogen Mixing

Initially, molecular hydrogen was mixed with the flow to enhance the Lyman series for spectra identification. The visible plasma plume, which turned brilliant red, was quenched beyond approximately 10 cm downstream of the orifice. Spectra observed 7.5 cm downstream of the orifice included the many-lined spectrum of the hydrogen molecule, the first six lines of the Lyman series of the hydrogen atom, and the usual contaminant radiation. No hydrogen continuum radiation was observed. The intensity of the Lyman H_α line was greatly increased. This line was observed under all conditions of plasma flow, was investigated, and consequently, furnished a reference point on all film.

4.3.2 Nitrogen Mixing

Introducing molecular nitrogen into the periphery of the argon plasma resulted in the appearance of additional nitrogen lines as well as the enhancement of the usual contaminant N lines. All of the N lines observed from the nitrogen plasma were present. Further, the molecular nitrogen itself was excited and gave rise to the Lyman-Birge-Hopfield band system. Sixteen bandheads were observed. All were members of v'' progressions with upper states $v' = 0$, $v' = 1$, and $v' = 2$ (Table II). The most intense bands were those of the v'' progression with $v' = 0$: (0, 1), (0, 2), (0, 3), (0, 4), and (0, 5). Of these the (0, 2) and (0, 3) bands contained the most rotational structure and were slightly more intense than the others. Visually, the normally pink argon plasma changed to light orange in color.

4.3.3 Carbon Dioxide Mixing

When carbon dioxide was mixed with the argon plasma, the plume turned a pale green, and extremely intense VUV radiation was emitted. Normally, exposures of 10 min were required to obtain data, but with this intense radiation, exposure times as short as 5 sec were ample. The intense radiation was identified as the fourth positive band system of carbon monoxide. Some 20 bandheads were observed (Table III). All the normal contaminant radiation occurred in the 5-sec exposures, but the argon resonance lines were much reduced in intensity and could be observed only by longer exposures.

4.3.4 Oxygen Mixing

Mixing molecular oxygen into the boundary of the argon plasma resulted in a plume which was lighter in color and smaller in diameter than the normal argon plume. The atomic oxygen resonance triplet at 1302, 1304, and 1306 Å was considerably enhanced to the extent that these lines appeared to be self-absorbed. Over 20 additional O lines were observed under these conditions. All these except two are the results of upper excited states decaying directly to the ground state (Fig. 10). The other two, which are relatively weak lines, have a final state in the two metastable levels at 1.93 and 4.19 ev, respectively. No molecular oxygen radiation was observed; however, the usual contaminant (carbon, nitrogen, hydrogen) radiation was present.

4.3.5 Helium Mixing

Adding helium around the plume had no effect on the argon plasma except that all lines appeared to be more intense. This was attributed to the reduction of ambient gases in the test cell that absorb a portion of the radiation emitted by the plasma.

4.4 LOCALIZED STUDIES

The work described to this point involved viewing the radiation across the entire gaseous stream. In this section are described observations made in three regions within the flow: (1) the outer region, which should consist primarily of the ambient test cell gases, (2) the boundary region, where the plasma mixing with these ambient gases is predominant, and (3) the core region consisting primarily of argon plasma. In the outer region, no radiation was observed during a 20-min exposure. In the boundary region, atomic radiation of all the contaminant species except carbon occurred; however, 10-min exposures revealed no trace of the argon resonance lines or of the higher frequency argon lines. Spectra obtained from the core of plasma flow showed only three very weak atomic nitrogen lines, the Lyman H_α line, the oxygen triplet, and the resonance lines of argon. The higher frequency lines of argon did not appear in the core region, probably because the exposure time was too short. When nitrogen was introduced into the periphery, the core spectra underwent these changes: the two sets of N doublets at 1493 and 1743 Å were greatly enhanced, and the N triplet at 1200 Å appeared; at the same time, the argon resonance lines disappeared. It should be pointed out that these experiments were done only once and rather crudely. A more refined way of viewing various regions of the plasma flow is required to make meaningful interpretations of these results. However, it appears that the excitation mechanisms are different in different regions of the flow.

SECTION V
ANALYSIS OF EXPERIMENTS

Data from the mixing studies provided some insight into the energy transfer mechanisms occurring in the plasma. Although the results are not yet conclusive, several alternative mechanisms suggested and supported by the data are discussed.

At the operating pressures at which these studies were made, the excitation mechanisms are assumed to be collisional rather than radiative. This is supported by the results of the zone (localized) experiments in which radiation did not occur outside the mainstream of the plume, indicating that collisions with particles in the plume were necessary for excitation. Thus, the resonance absorption suggested by Bowen (Ref. 3) does not seem to be a factor. The observed radiation may be explained by attributing the excitation to collisions of the second kind involving an argon energy carrier. These collisions are thought to be three-body collisions (Ref. 9) involving an argon metastable atom or an argon ion, an electron, and an atom or molecule of the foreign gas. Previous experiments have indicated a typical gas number density of 6×10^{16} cm^{-3} and an ion number density of 2×10^{14} cm^{-3} (Ref. 10). Under these conditions, the gas model suggested by Brewer (Ref. 11) predicts a metastable atom density of 10^{10} cm^{-3}. Three possible types of energy transfer are suggested by the measurements: (1) direct excitation of molecules in a single collision followed by band radiation, (2) a two-collision process in which dissociation to a ground-state atomic species occurs in the initial collision followed by atomic excitation in the second collision with subsequent line radiation, and (3) dissociation by collision directly to an excited species and subsequent radiation. The roles played by these mechanisms are discussed in detail for each foreign gas.

Allowing hydrogen gas to mix into the periphery of the argon plasma resulted in the enhancement of the H_α line, the appearance of several other atomic hydrogen lines of the Lyman series, and the Lyman band (many-line spectrum) of molecular hydrogen. The H_α line is probably enhanced as a consequence of a three-body collision involving an electron, an argon ion, and a hydrogen molecule. The molecule is dissociated into a ground-state atom and an excited atom which subsequently decays to the ground state by emission of the Lyman H_α line. Symbolically,

$$H_2 + A^- + e \longrightarrow H^* (^2P, 10.18 \text{ ev}) + H + A$$

$$H^* (^2P) \longrightarrow H + h\nu (H_\alpha, 1215 \text{ Å})$$

where the superscript (+) indicates an ionized particle and the superscript (*) indicates an excited state. The recombination of $A^+ + e$ provides 15.7 ev, of which approximately 4.5 ev is required to dissociate the hydrogen molecule, and 10.18 ev provides the energy to excite one of the hydrogen atoms to the ^2P level from which Lyman alpha originates.

It is further suggested that the upper states from which the other emission lines of the Lyman series originated are excited by three-body collisions involving an argon metastable atom, a hydrogen atom, and an electron with an energy greater than 0.3 ev. The argon metastable can provide an energy of 11.55 or 11.72 ev in a collision of the second kind.

$$H + A^m \left(\tfrac{1}{2}\left[\tfrac{1}{2}\right]_0 \text{ or } \tfrac{3}{2}\left[\tfrac{3}{2}\right]_2\right) + e\,(KE > 0.3\text{ ev}) \longrightarrow H^* + A + e$$

$$H^* \longrightarrow H + h\nu \qquad \text{(additional lines of the Lyman series)}$$

where the superscript (m) indicates a metastable state. The ^2P level of hydrogen can also be excited by this mechanism except that the electron must carry off energy rather than furnish it in this case. Another explanation of the appearance of this series is the collision of a metastable argon atom, an electron, and a hydrogen atom exciting the hydrogen to its metastable level of approximately 10.2 ev, where a collision of an energetic electron with the metastable hydrogen atom could excite it into one of the upper states;

$$H + A^m + e \longrightarrow H^m\ (10.2\text{ ev}) + A + e$$

$$H^m + e \longrightarrow H^* + e$$

$$H^* \longrightarrow H + h\nu \qquad \text{(all possible lines of the Lyman series)}$$

The appearance of the many-line spectrum of H_2 is best explained by the three-body collision of the molecular hydrogen with a metastable argon atom and an electron;

$$H_2 + A^m + e \longrightarrow H_2^*\ (14.5 \text{ to } 7.5\text{ ev}) + A + e$$

$$H_2^* \longrightarrow H_2 + h\nu$$

The limited energy available in the argon metastable is the reason for not observing the many-line spectrum below 1150 Å. This spectrum has been observed as low as 850 Å (Ref. 12). The primary purpose of

the electron in this reaction is to act as an energy reservoir so that the hydrogen atom may accept the exact energy necessary for one of the allowable excited states.

The nitrogen mixing, experimentally similar to hydrogen mixing, produced both atomic line radiation and molecular band radiation. The atomic line radiation was attributed to the dissociation of the molecular nitrogen in a three-body collision with a recombining argon ion and an electron;

$$N_2 + A^+ + e \longrightarrow N\ (^2D) + N\ (^2D) + A$$

To energetically balance this equation, the nitrogen atoms are assumed to be in the ^2D metastable state, each having an energy of 2.38 ev above the ground state. These nitrogen atoms then could be excited in a three-body collision with an argon metastable and electron, with the resultant observed line radiation produced as the excited states decay;

$$N\ (^2D) + A^m + e \longrightarrow N^*\ (10.9 \text{ to } 7.1 \text{ ev}) + A + e$$

$$N^* \longrightarrow N + h\nu \qquad \text{(N line radiation)}$$

The Lyman-Birge-Hopfield bands of molecular nitrogen are believed to be excited by the following three-body collision:

$$N_2 + A^m + e \longrightarrow N_2\ (a'^1\Pi_g^{'},\ 11.0 \text{ to } 8.5 \text{ ev}) + A + e$$

where the prime indicates vibrational excitation. This requires that about 2.5 ev be carried off by the three bodies as translational energy. At this time, the possibility that the upper levels of the Lyman-Birge-Hopfield bands are populated in the following manner cannot be ruled out:

$$N_2 + A^+ + e \longrightarrow N_2^+\ (^2\Sigma_g^+,\ 15.7 \text{ ev}) + A + e$$

$$N_2^+\ (^2\Sigma_g^+) + e + e \longrightarrow N_2^*\ (14.3 \text{ to } 12.5 \text{ ev}) + e$$

$$N_2^* \longrightarrow N_2\ (a'^1\Pi_g) + h\nu$$

$$N_2\ (a'^1\Pi_g) \longrightarrow N_2 + h\nu \qquad \text{(Lyman-Birge-Hopfield Band System)}$$

This is, however, a three-step process which makes it less likely than the straightforward single step involving A^m.

The intense radiation which appears on mixing carbon dioxide into the argon plasma is identified as the fourth positive band system of carbon monoxide. The most satisfactory explanation for the excitation

of the CO to the $A^1\Pi$ electronic state from which this emission system originates appears to be a three-body collision involving the argon ion;

$$CO_2 + A^+ + e \longrightarrow CO\ (A^1\Pi,\ 10.8\ \text{to}\ 8.2\ ev) + O\ (^1D,\ 1.97\ ev) + A$$

followed by the radiation transition

$$CO\ (A^1\Pi) \longrightarrow CO\ (^1\Sigma) + h\nu \qquad \text{(Fourth Positive Band System)}$$

The evidence for this reaction is twofold: first, the radiation is extremely intense, indicating that the excitation is very fast and requires a large number of collisions; second, the atomic oxygen is left in a metastable state so that it does not contribute substantially to oxygen resonance line intensity. It was observed that the oxygen 1300-Å lines are not enhanced with the addition of CO_2.

However, the atomic carbon lines (Fig. 11) are enhanced with CO_2 addition. This may be explained by the following process:

$$CO + A^+ + e \longrightarrow C + O\ (^1S,\ 4.19\ ev) + A$$

$$C + A^m - e \longrightarrow C^* + A + e$$

$$C^* \longrightarrow C + h\nu \qquad \text{(C line radiation)}$$

The dissociation of the CO requires 11.1 ev which, together with the 4.19 ev to excite the O to the metastable ^1S state, leaves only about 0.4 ev of the 15.7 ev provided by $A^+ + e$ to be distributed as translational energy. Other reactions in which the carbon atom and the oxygen atom share the excess energy are possible, provided each goes to a metastable state. Reactions which lead to atomic oxygen going to the ground state are not likely, however, because there is no enhancement of the oxygen resonance lines at 1300 Å. The atomic carbon is now excited to high electronic levels by collisions, probably with a metastable argon as shown above.

Mixing molecular oxygen into the boundary of the argon plasma results in considerable enhancement of the OI resonance triplet 1302, 1304, and 1306 Å. The enhancement of this triplet can be readily explained on the basis of the following reaction:

$$O_2 + A^+ + e \longrightarrow O\ (3s\ ^3S_o) + O\ (^3P) + A$$

The argon ion recombination again provides 15.7 ev, of which 5.0 ev are required to dissociate the oxygen and an additional 9.5 ev place one of the atoms in the excited state $3s\ ^2S_o$. The other atom goes to the ground state, and the remaining energy is distributed as translational energy among the products. Over 20 other lines were observed

on this occasion and can probably be attributed to the excitation of atomic oxygen in the ground state to very high excited states (about 12 to 13 ev), including the upper level of the resonance lines ($3s\ ^3S_o$), from which it subsequently decays to various lower levels, the metastable levels (^1S and ^1D), and the ground state. This excitation may result from a three-body collision of atomic oxygen with an argon metastable atom and an energetic electron. Thus,

$$O + A^m + e \longrightarrow O^* \text{ (12 to 13 ev)} + A + e$$

It would appear that the argon ion cannot play a role in this atomic excitation process because it provides sufficient energy to ionize rather than excite the oxygen.

SECTION VI
DISCUSSION

The primary purposes of this investigation were to develop experimental techniques of VUV spectroscopy in a test cell environment, to map the radiation emitted from an arc-jet plasma in the VUV spectral region, and to determine excitation-radiative mechanisms where possible. These goals were largely achieved.

6.1 DEVELOPMENT AND MEASUREMENT TECHNIQUE

The attainment of high vacuum is the usually preferred method of making spectral measurements in the VUV region. This involves differential pumping in the presence of flowing gases. The experiments reported on herein have demonstrated that a purging technique using helium as the purge gas gives satisfactory results for exploratory work. Helium flows throughout the optical path with the possible exception of approximately 6 cm extending from the window of the test cell to the gas stream. If the air in the optical path could be completely replaced by helium, then the optical path would be transparent to all radiation between 2000 and 600 Å. It is believed that the flowing purge technique used here is effective to 600 Å, but this cannot be proved at this time. Spectra have been observed to 790 Å.

One run was made without a flowing purge. In this case, only the oxygen triplet at 1300°A, the hydrogen alpha line, one of the nitrogen lines at 1200 Å, two nitrogen lines at 1742 Å, and one carbon line at 1931 Å were observed. This indicates that, even though helium fills

the spectrograph tank, without a flowing purge considerable efficiency in the ability to observe radiation from the plasma is lost. There is some leakage of air into the tank; this would account for at least some of the absorption of the emitted radiation. It should be noted that there is a window in the atmosphere between 1200 and 1350 Å. This would account for the observance of the emitted radiation of the nitrogen line at 1200 Å, the hydrogen line at 1215 Å, and the oxygen triplet at 1300 Å. The nitrogen doublet that appears at 1742 Å occurs in the Schumann Runge absorption system, a band system, and in order for it to be reabsorbed, it would have to have a resonant transition with the oxygen. Apparently, it does not have. The same thing can be said about the carbon line at 1931 Å.

One other comment on the effectiveness of the purge can be made. Below 1100 Å, almost all of the constituents of the atmosphere begin absorbing very strongly. The fact that anything at all could be observed in this region, and spectra were observed as low as 790 Å, is good indication that the purging technique developed here is quite efficient. It is felt that this is a very effective means of eliminating atmospheric absorption. A rather simple, inexpensive shelf item, mainly the Cenco spectrograph, was used to develop a highly effective instrument for plasma spectra identification in the VUV region. This is something which can be useful in many laboratories where a highly elaborate instrumentation setup is not available.

6.2 SPECTRAL MAPPING

Another aim of this program was to map the radiation in the VUV region from a low-density plume of arc-jet-produced plasma. This mapping called for a classification of spectra, the location of the spectral elements along the wavelength scale, the measurement of relative intensities, and the determination of the excitation energies involved within the plasma. It was possible to classify the spectra as to atomic, molecular, or ionic origin. In addition to classifying the spectra, the individual components have been identified as being emitted by a particular species such as atomic hydrogen, atomic nitrogen, atomic oxygen, molecular nitrogen, molecular hydrogen, and molecular oxygen. All of the observed spectra were located along the wavelength scale between 2000 and 700 Å. This is summarized in Table I for the convenience of other investigators who may want to explore this region.

Little effort was devoted to measuring relative intensities at this time because of the difficulties of making intensity measurements from

film. An additional problem in the VUV is the unavailability of a standard intensity source. Some effort was made to determine relative intensities by comparing the intensity calibrations which other investigators have obtained for a film similar to the film used here. It was found, however, that the data scattering for this type of comparison was such as to make any intensity values invalid. The most that can be said about intensities is that the observed spectra could be characterized by their intensity in that some lines are invariably strong, whereas others are always weak.

6.3 EXCITATION-RADIATION MECHANISMS

The third objective of the experiments was to determine possible excitation mechanisms that must take place in the plasma. The approach here was to examine the energy levels corresponding to the observed transition. If these transitions take place, there must have been some mechanism, probably collisional, possibly radiative, which caused the atoms and molecules to be populated in highly excited states. By determining the states from which the transitions originate, the energy required to raise the species to that excited level could be evaluated. Then some mechanism within the plasma was sought which could provide the required amount of energy. These postulated energy transfer mechanisms have been discussed. It has been postulated previously (Ref. 6) from visible spectra that collisions of the second kind play a major role in exciting species in argon plasmas produced in the manner studied here. However, it was believed that the argon metastable atom played the major role. The most interesting new evidence in this regard is the possible important role played by three-body collisions involving the argon ion, and electron, and the species to be excited. This is evidenced by the observed excitation which can be explained only on the basis of an energy carrier with considerably more energy than is possessed by the metastable atom. Thus, the argon ion appears to be as effective an energy reservoir as the argon metastable atom in these plasmas. Finally, it was definitely demonstrated that resonance absorption does not play an important role in the excitation process since no VUV radiation is observed in regions where collisional activity with energy carriers is not present.

6.4 UNEXPLAINED PHENOMENA

Several factors have been left unresolved by these results. It was thought that the expected large population of argon atoms in metastable states would be revealed by the appearance of the forbidden spectral

lines. The fact that these did not appear only means that the transition probability is very small. A different experiment is required to establish the level of population of the metastable states. The resonance levels were found to be well populated, since resonance lines were strong, but the absolute population must await absolute intensity measurements. The appearance of many lines originating in upper states will provide an excellent measure of the population distribution of the excited states in argon, once intensity measurements are made.

Another factor which requires further study is the absence of the Vegard-Kaplan bands while the Lyman-Birge-Hopfield bands appear quite strongly when nitrogen is added. Previous measurements in other spectral regions (Ref. 6) had shown that the second positive ($C^3\Pi \rightarrow B^3\Pi$) system was very strong, and the first positive system ($B^3\Pi \rightarrow A^3\Sigma$) was also present. Thus, the Vegard-Kaplan system $A^3\Sigma \rightarrow X^1\Sigma$) would be expected, since its upper state is being continuously populated. Instead, the Lyman-Birge-Hopfield system ($a^1\Pi \rightarrow X^1\Sigma$) appeared. This requires further study.

REFERENCES

1. Brewer, L. E. and McGregor, W. K. "The Influence of Metastable Atoms on the Populaion of Excited States in a Thermal Plasma." Proceedings of the Sixth International Symposium on Ionization Phenomena in Gases, Paris, France, July 1963.
2. Robben, F., Kunkel, W. G. and Talbot, L. "Spectroscopic Study of Electron Recombination with Monatomic Ions in a Helium Plasma." Physical Review, Vol. 132, No. 6, December 1963, p. 2363.
3. Bowen, S. W. "Spectroscopic and Optical Studies of a High Pressure, Underexpanded Jet." AIAA-66-164.
4. Dooley, M. T., McGregor, W. K. and Brewer, L. E. "Characteristics of the Arc in a Gerdien-Type Plasma Generator." AEDC-TR-61-13 (AD268410), December 1961.
5. Hunter, W. R. "High Reflectance Coatings in the Extreme Ultraviolet." Optica Acta, Vol. 9, No. 3, July 1962, pp. 255-258.
6. Brewer, L. E. and McGregor, W. K. "The Radiative Decay of Metastable Argon Atoms in a Low-Density Argon Plasma Stream." AEDC-TDR-63-5 (AD294543), January 1963; also "Excitation of Nitrogen by Metastable Argon Atoms." Physics of Fluids, Vol. 5, No. 11, November 1962, pp. 1485-1486.

7. Boyce, J. C. and Robinson, H. A. "Wave-Length Identification Lists for the Extreme Ultraviolet." Journal of the Optical Society of America, Vol. 26, No. 4, April 1936, p. 133.

8. Kelly, R. L. "Atomic Emission Lines below 2000 Angstroms, Hydrogen through Argon." NRL Report 6648, February 1968.

9. Herzberg, G. Molecular Spectra and Molecular Structure, I. Spectra of Diatomic Molecules. Second Edition, D. Van Nostrand Company, Inc., Princeton, New Jersey, 1964.

10. Boatman, R. "An Investigation of an Expression for the Conductivity of a Low-Density, Free-Jet, Arc-Heated Plasma." M. S. Thesis, The University of Tennessee, June 1968.

11. Brewer, L. E. "Plasma Radiation Resulting from an Over-Population of Atoms in the Metastable State." M. S. Thesis, The University of Tennessee, March 1965.

12. Bates, D. R. and Estermann, I., Ed. Advances in Atomic and Molecular Physics. Academic Press, New York, 1966.

13. Cowan, R. D. and Andrew, K. L. "Coupling Considerations in Two-Electron Spectra." Journal of the Optical Society of America, Vol. 55, No. 5, May 1965, pp. 502-516.

14. Lofthus, A. "The Molecular Spectrum of Nitrogen." Spectroscopic Report No. 2, Department of Physics, University of Oslo, Blindern, Norway, December 1960.

15. Krupenie, P. H. "The Band Spectrum of Carbon Monoxide." NSRDS-NBS 5, July 1966.

APPENDIXES

I. ILLUSTRATIONS
II. TABLES

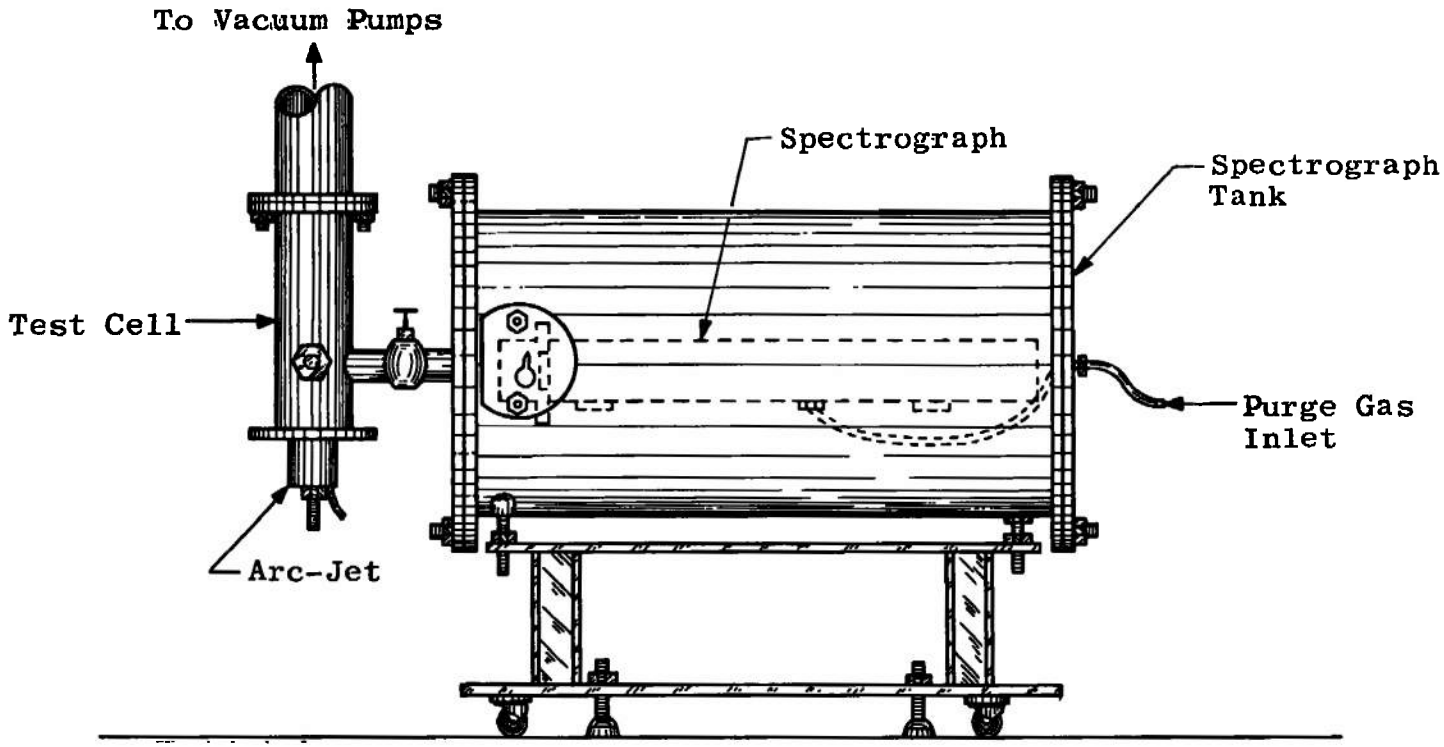

Fig. 1 Arc-Jet, Test Cell, and Spectrographic Apparatus

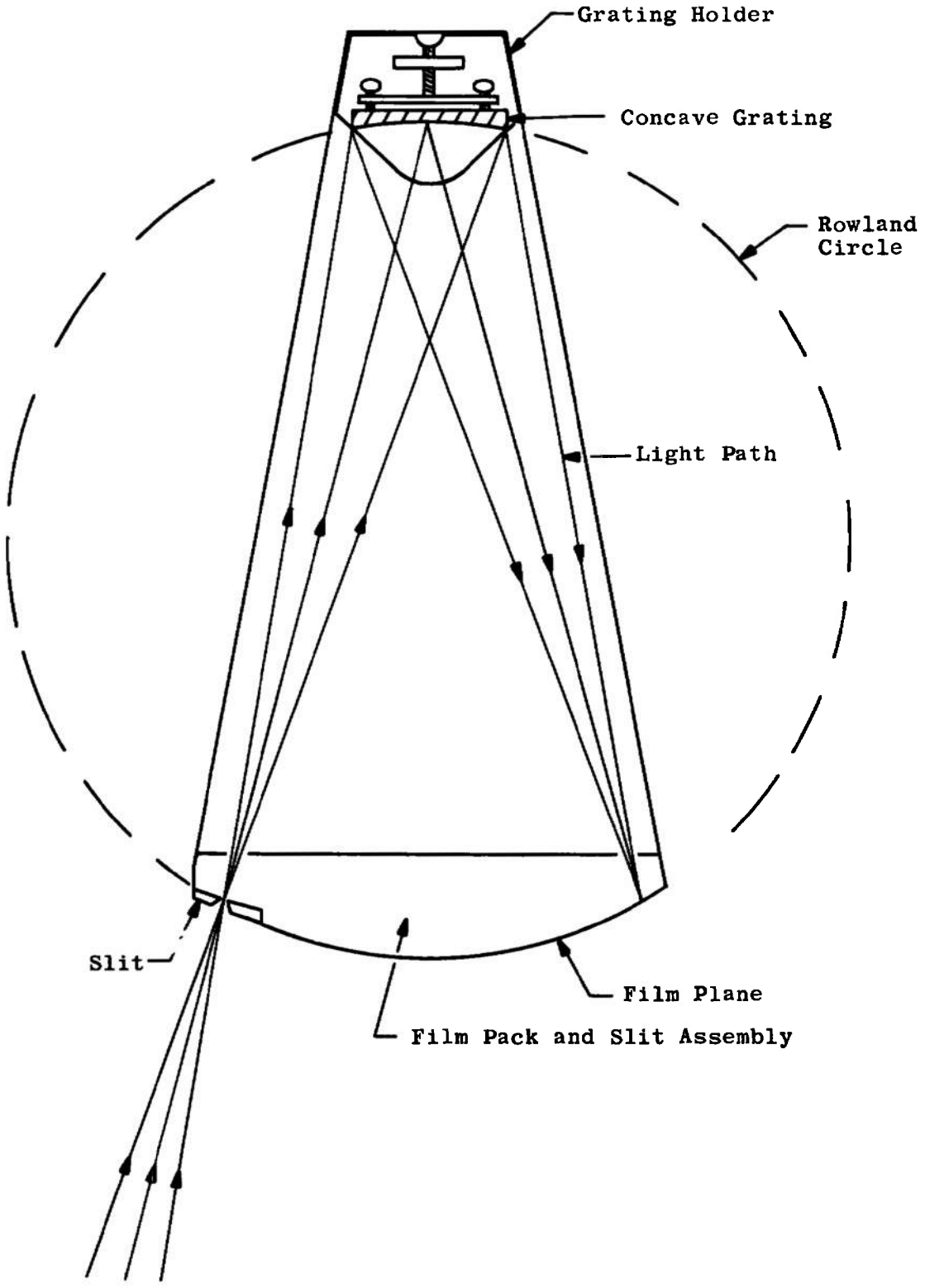

Fig. 2 Paschen/Runge Mount Spectrograph

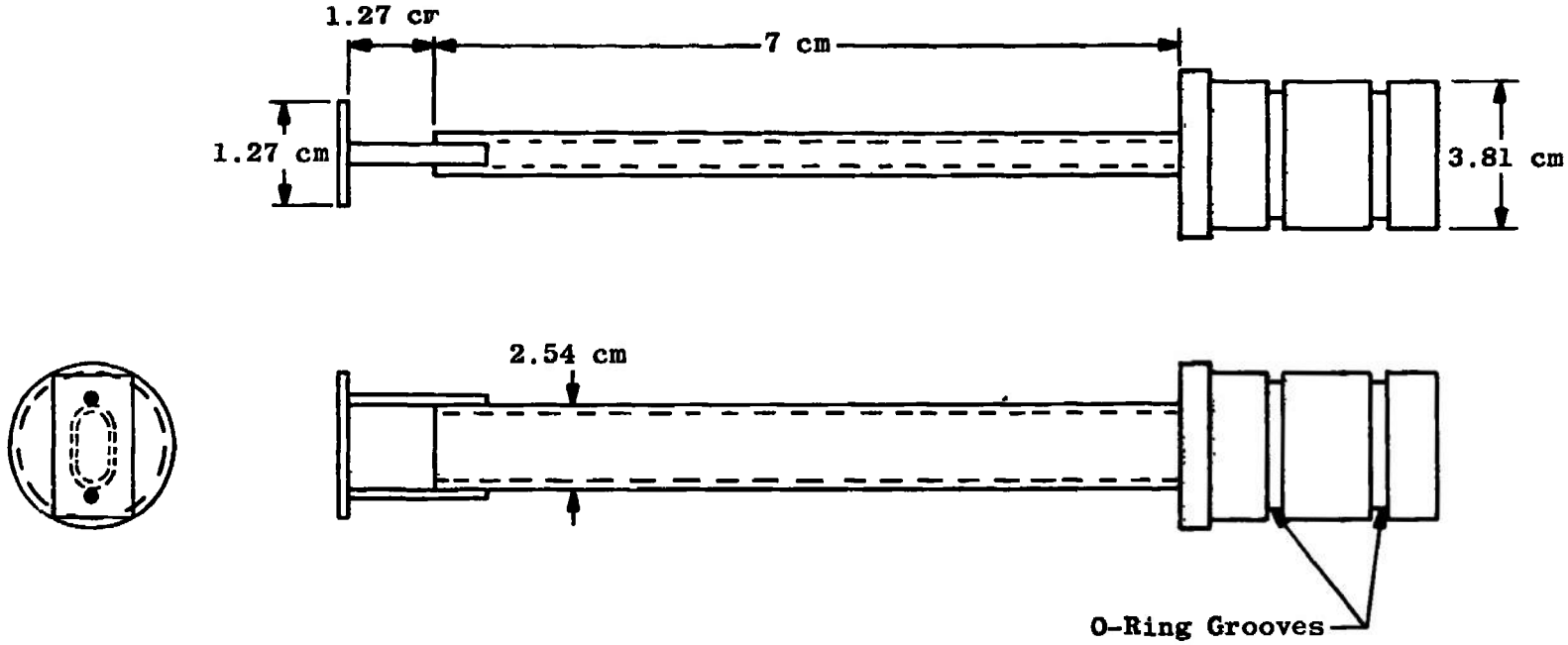

Fig. 3 Viewing Tube

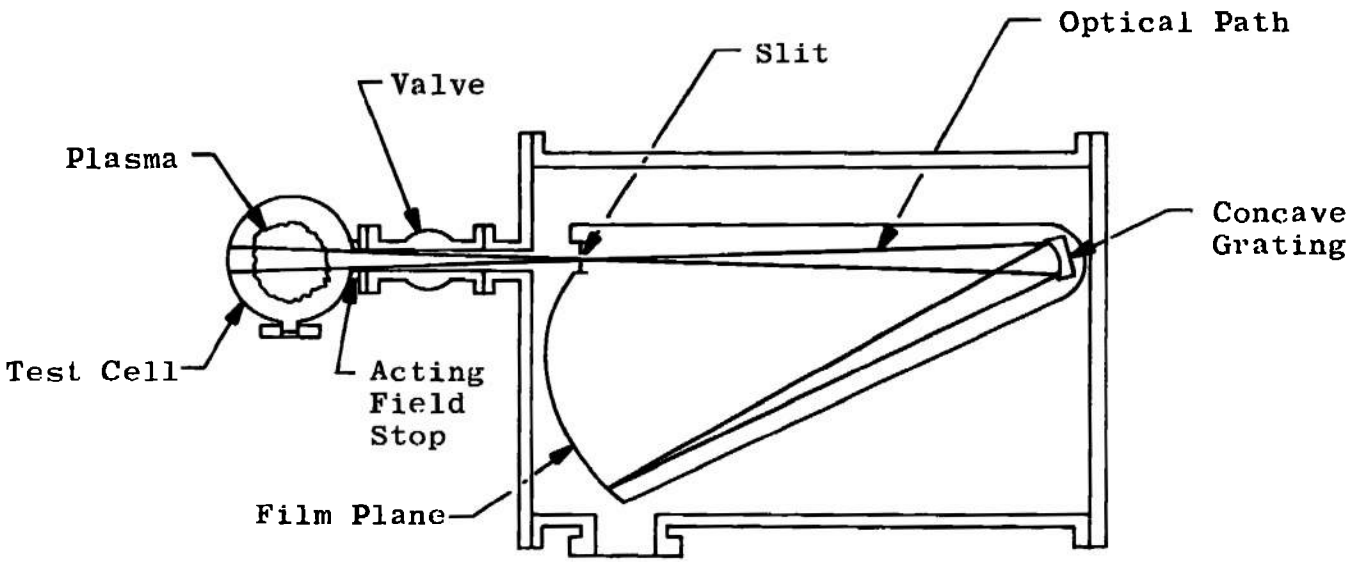

Approximately 1/10 Scale

Fig. 4 Optical Path

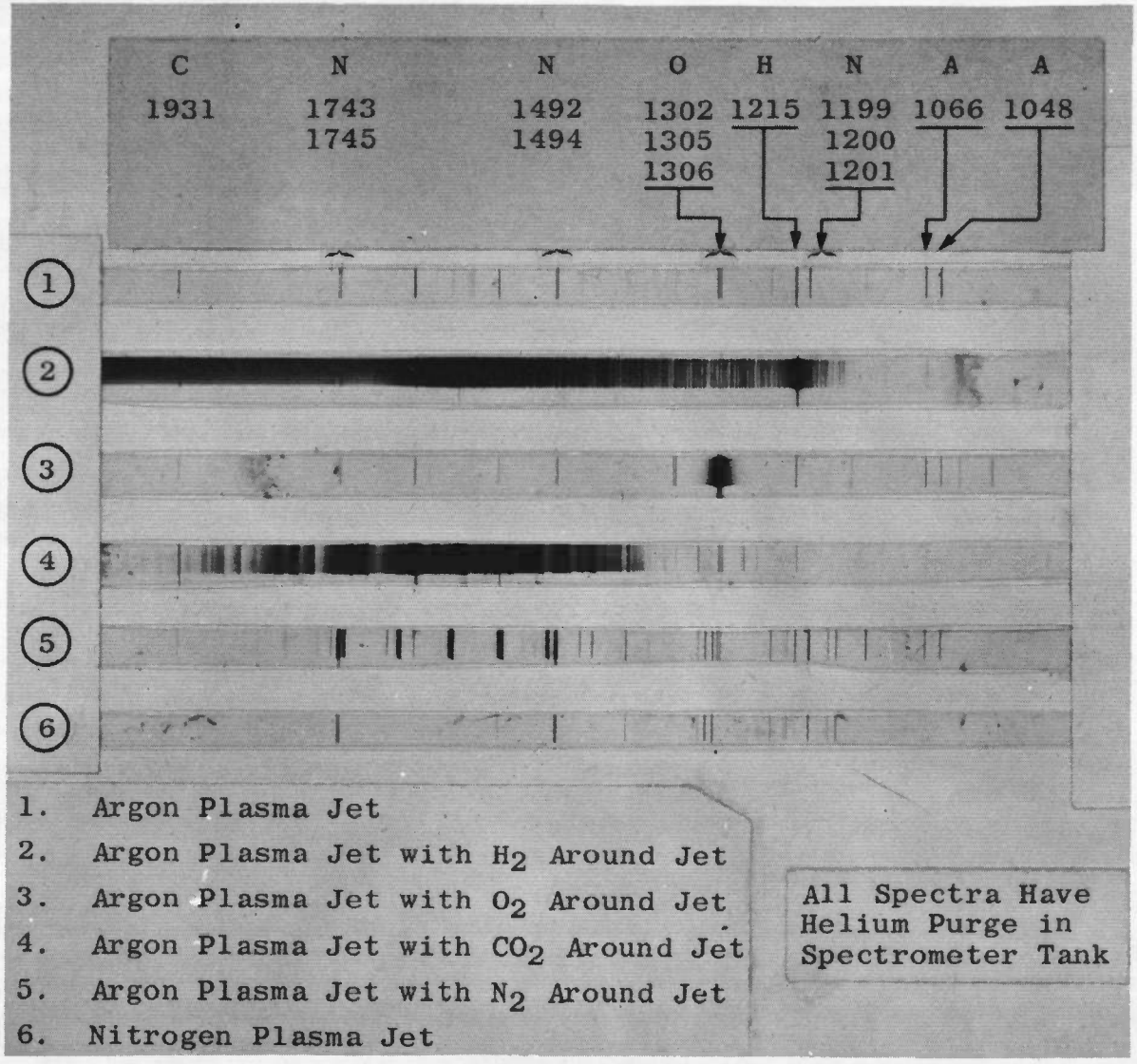

Fig. 5 Typical Spectrographic Film Strips

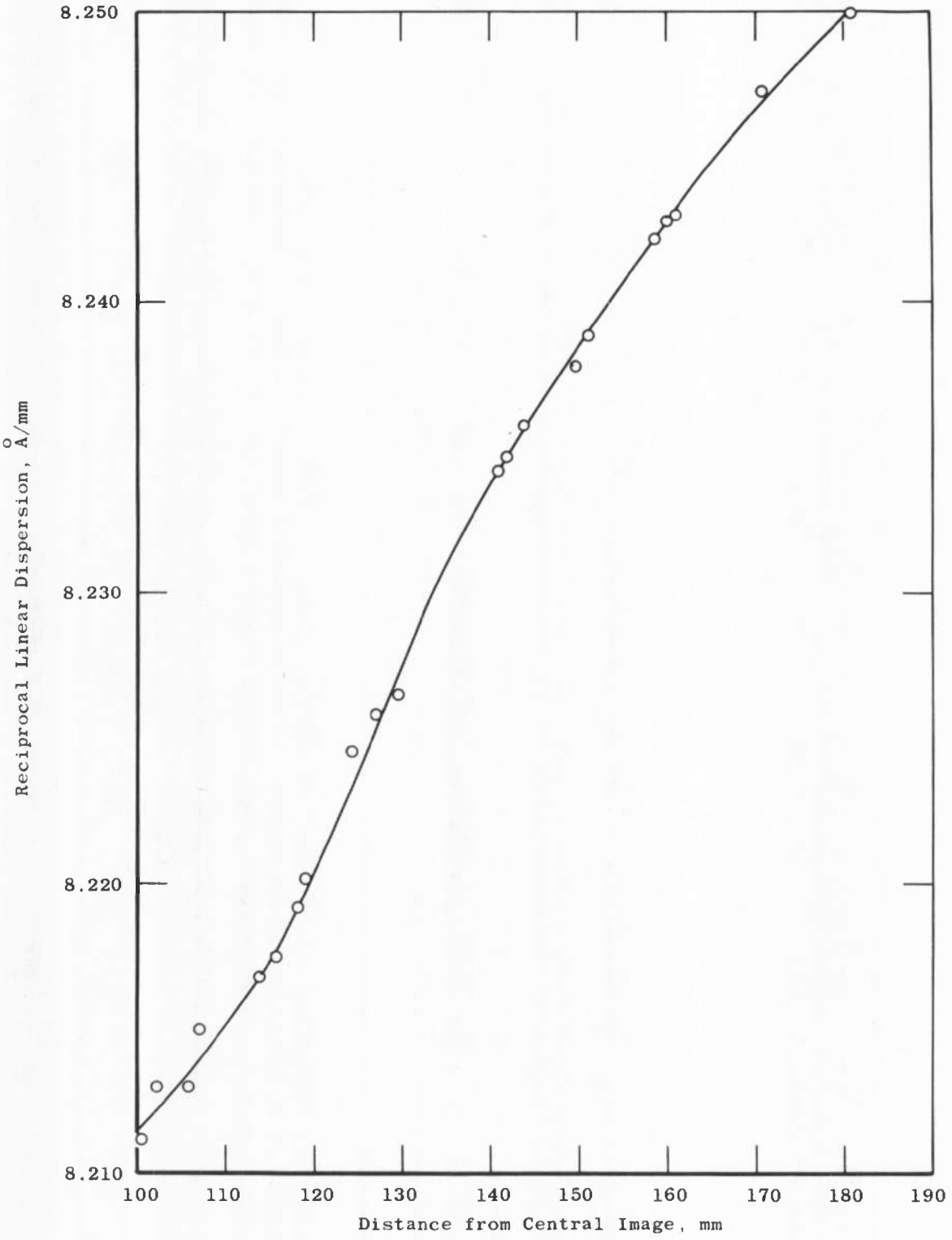

Fig. 6 Dispersion Curve

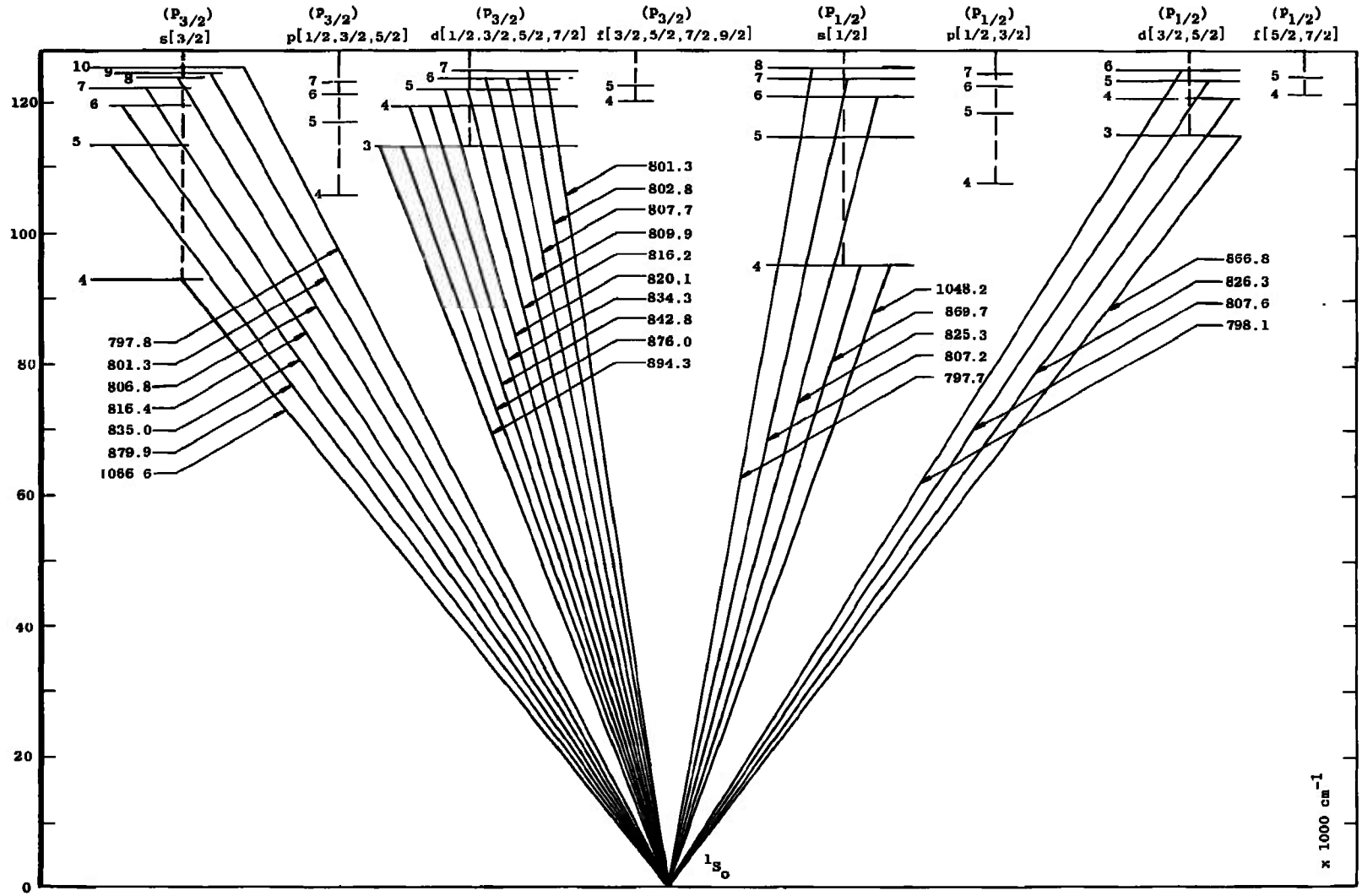

Fig. 7 Term Diagram of Argon

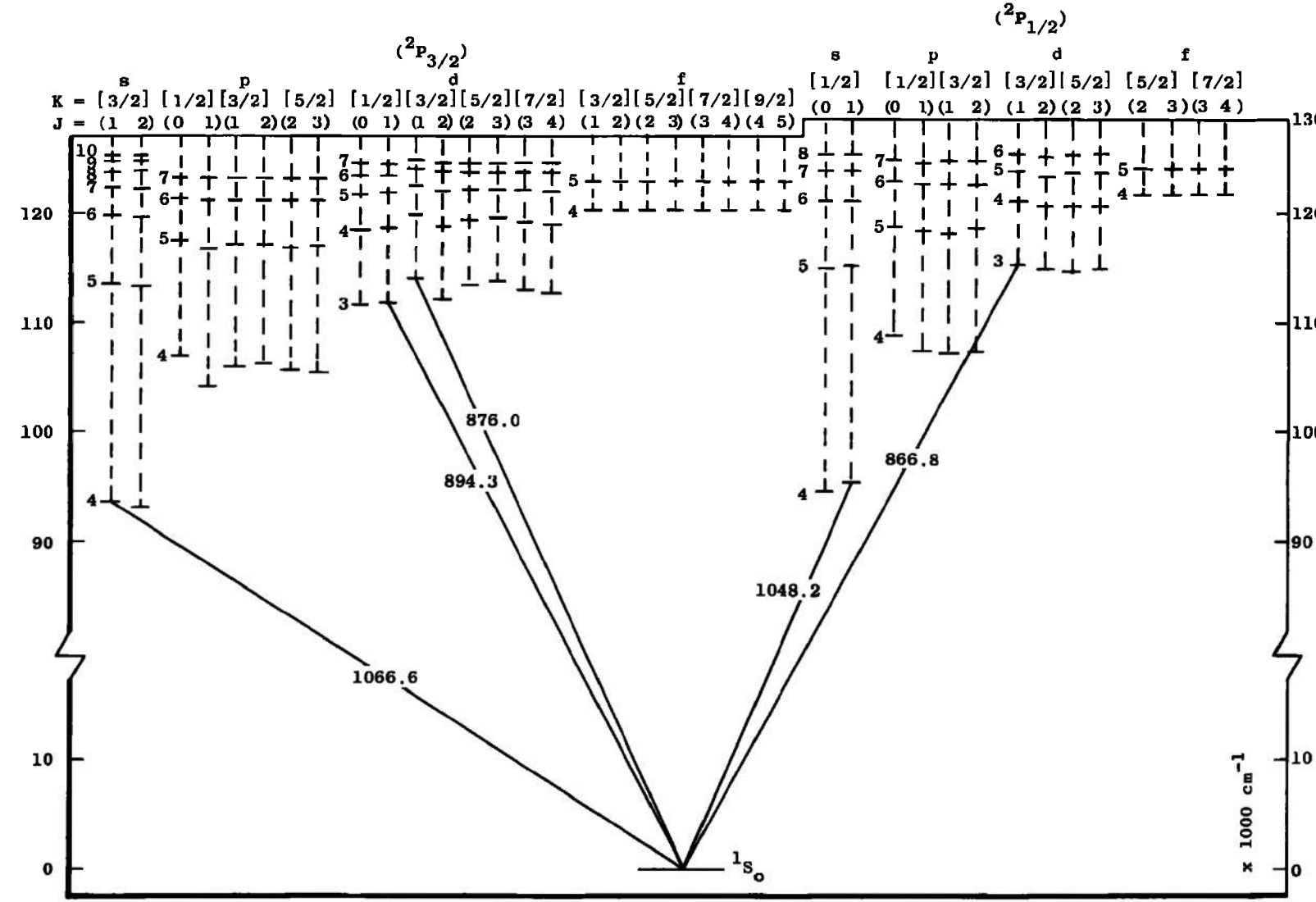

Fig. 8 Term Diagram of Argon (Fine Structure)

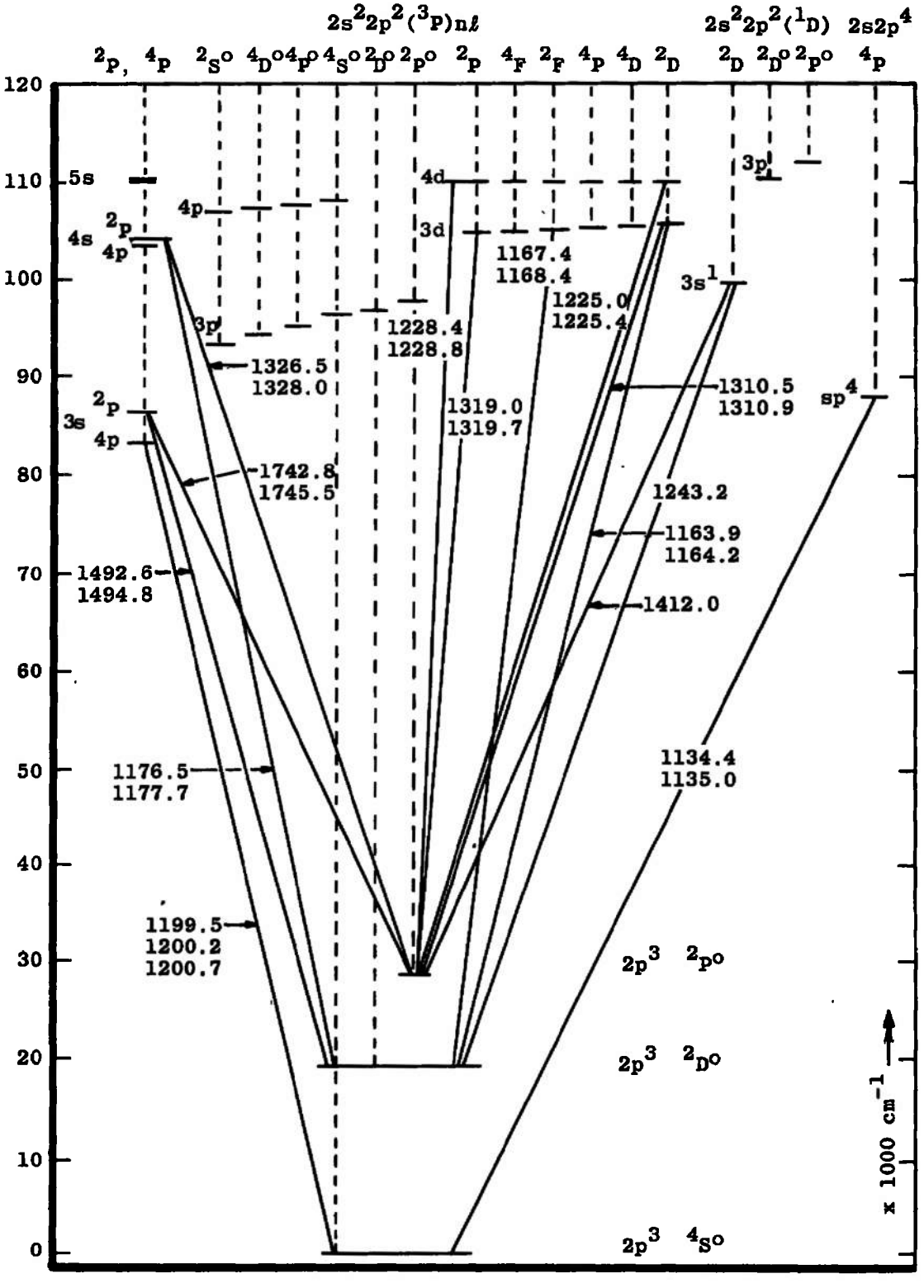

Fig. 9 Term Diagram of Nitrogen

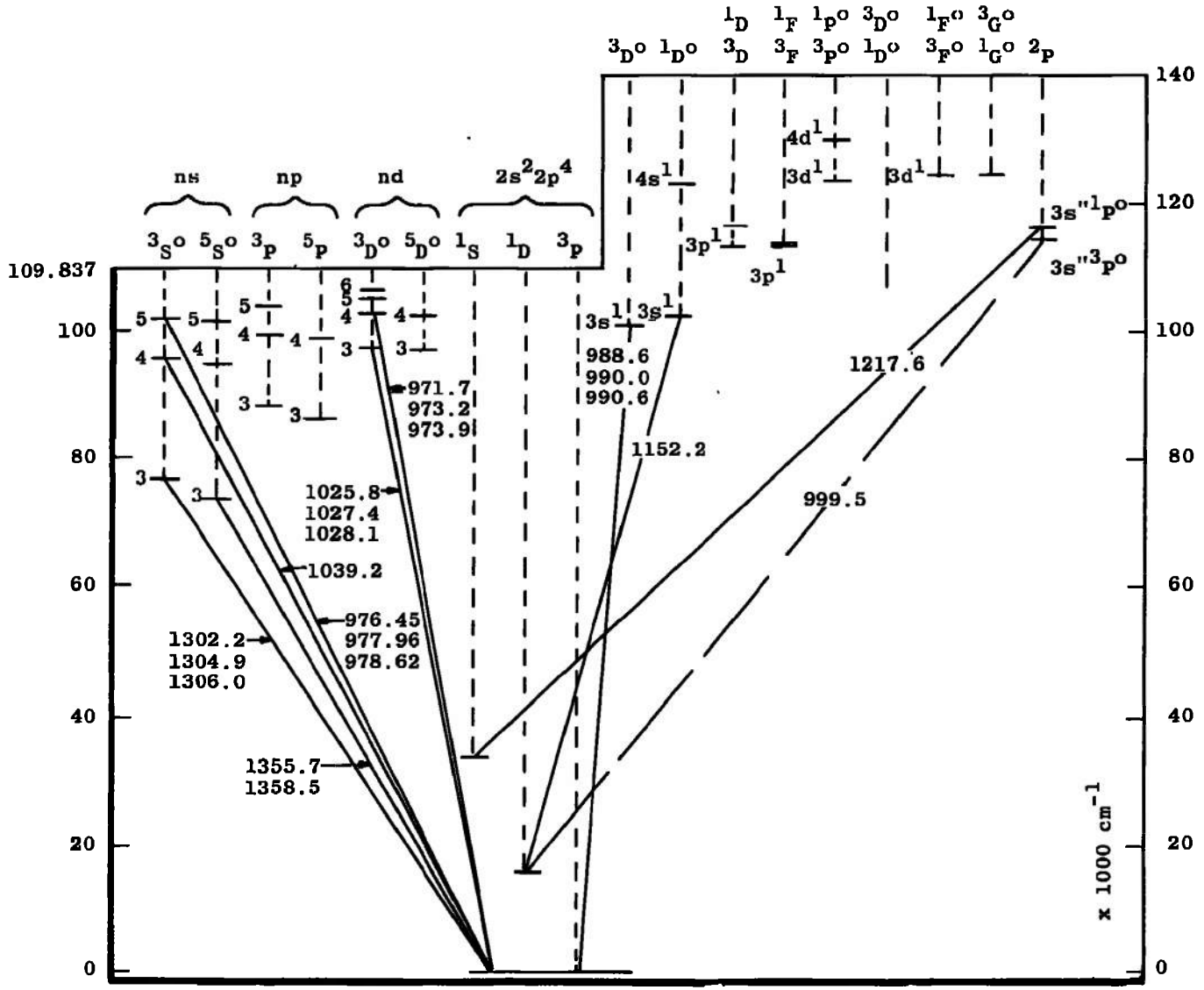

Fig. 10 Term Diagram of Oxygen

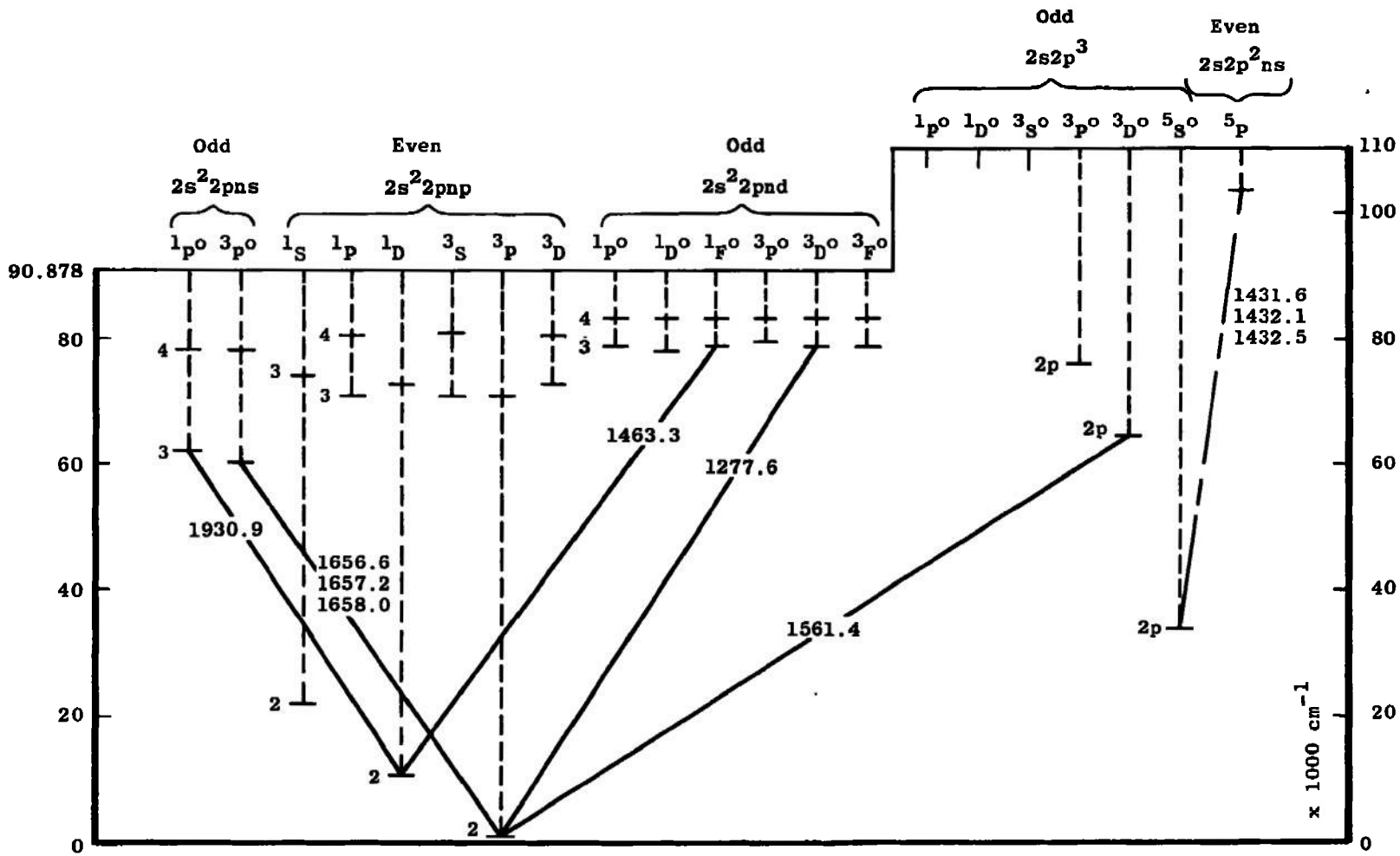

Fig. 11 Term Diagram of Carbon

TABLE I

OBSERVED VUV WAVELENGTHS AND TRANSITIONS FOR ATOMIC A, H, N, O, AND C AND MOLECULAR N_2 (L-B-H) AND CO (FOURTH POSITIVE)

The jK coupling scheme (Ref. 13) is described as the coupling of the orbital angular momentum (ℓ_1) and spin (s_1) of the screening electrons to form an angular momentum (j), which couples to the orbital angular momentum of the excited electron (ℓ_2) to form the resultant angular momentum quantum number (K). K then couples with the spin of the excited electron (s_2) to form the total angular momentum quantum number (J). Thus, schematically

Type of Coupling	Description	Notation
jK	$\left[\{(\ell_1, s_1)\ j_1, \ell_2\}\ K, s_2\right] J$	$j_1[K]\ J$

This jK coupling is used for the argon lines listed, and the LS coupling scheme is used for the nitrogen, oxygen, hydrogen, and carbon lines listed. The number in parentheses beside a molecular listing is the appropriate vibrational bandhead nomenclature (v' [upper vibrational quantum number], v'' [lower vibrational quantum number]). The N_2 designation refers to the Lyman-Birge-Hopfield system of molecular nitrogen, and the CO refers to the fourth positive system of carbon monoxide. The wavelengths for the atomic line radiation were taken from Ref. 8. The wavelengths for the bandheads of the Lyman-Birge-Hopfield system of molecular nitrogen were taken from Ref. 14, and the wavelengths for the bandheads of the fourth positive system of carbon monoxide were taken from Ref. 15.

TABLE I (Continued)

VUV Wavelength of Emitted Radiation, Å	Emitting Species	Upper State	Lower State
(797.75	A	$3p^5(^2P)$ 8s [1/2]$_1$	$3p^6$ $^1S_0$
797.88)	A	10s [3/2]$_1$	$^1S_0$
798.17	A	6d [3/2]$_1$	$^1S_0$
(801.36	A	9s [3/2]$_1$	$^1S_0$
801.39)	A	7d [3/2]$_1$	$^1S_0$
802.86	A	7d [1/2]$_1$	$^1S_0$
(806.88	A	8s [3/2]$_1$	$^1S_0$
807.22)	A	7s [1/2]$_1$	$^1S_0$
(807.65	A	5d [3/2]$_1$	$^1S_0$
807.70)	A	6d [3/2]$_1$	$^1S_0$
809.93	A	6d [1/2]$_1$	$^1S_0$
(816.23	A	5d [3/2]$_1$	$^1S_0$
816.47)	A	7s [3/2]$_1$	$^1S_0$
820.13	A	5d [1/2]$_1$	$^1S_0$
825.35	A	6s [1/2]$_1$	$^1S_0$
826.36	A	4d [3/2]$_1$	$^1S_0$
834.39	A	4d [3/2]$_1$	$^1S_0$
835.00	A	6s [3/2]$_1$	$^1S_0$
842.81	A	4d [1/2]$_1$	$^1S_0$
866.81	A	3d [3/2]$_1$	$^1S_0$
869.75	A	5s [1/2]$_1$	$^1S_0$
876.06	A	3d [3/2]$_1$	$^1S_0$
879.95	A	5s [3/2]$_1$	$^1S_0$
894.31	A	3d 1/2]$_1$	$^1S_0$

TABLE I (Continued)

VUV Wavelength of Emitted Radiation, Å	Emitting Species	Upper State	Lower State
926.23	H	$8p\ (^2P_{3/2})$	$1s\ (^2S_{1/2})$
930.75	H	$7p\ (^2P_{3/2})$	$1s\ (^2S_{1/2})$
937.80	H	$6p\ (^2P_{3/2})$	$1s\ (^2S_{1/2})$
949.74	H	$5p\ (^2P_{3/2})$	$1s\ (^2S_{1/2})$
971.74	O	$2s^2\,2p^3(^4S)\,4d\ ^3D$	$2p^4\ ^3P_2$
972.53	H	$4p\,(^2P_{3/2})$	$1s\ (^2S_{1/2})$
973.23	O	$2s^2\,2p^3(^4S)\,4d\ ^3D$	$2p^4\ ^3P_1$
973.88	O	$2s^2\,2p^3(^4S)\,4d\ ^3D_1$	$2p^4\ ^3P_0$
976.45	O	$2s^2\,2p^3(^4S)\,5s\ ^3S_1$	$2p^4\ ^3P_2$
977.96	O	$2s^2\,2p^3(^4S)\,5s\ ^3S_1$	$2p^4\ ^3P_1$
978.62	O	$2s^2\,2p^3(^4S)\,5s\ ^3S_1$	$2p^4\ ^3P_0$
988.58 988.65 988.77	O	$2s^2\,2p^3(^2D)\,3s\ ^3D_1$ $^3D_2$ $^3D_3$	$2p^4\ ^3P_2$ $^3P_2$ $^3P_2$
990.13 990.20	O	$2s^2\,2p^3(^2D)\,3s\ ^3D_1$ $^3D_2$	$2p^4\ ^3P_1$ $^3P_1$
990.80	O	$2s^2\,2p^3(^2D)\,3s\ ^3D_1$	$2p^4\ ^3P_0$
1025.76	O	$2s^2\,2p^3(^4S)\,3d\ ^3D$	$2p^4\ ^3P_2$
1025.72	H	$3p\ (^2P_3)$	$1s\ (^2S_{1/2})$
1027.43	O	$2s^2\,2p^3(^4S)\,3d\ ^3D$	$2p^4\ ^3P_1$
1028.16	O	$2s^2\,2p^3(^4S)\,3d\ ^3D$	$2p^4\ ^3P_0$
1039.23 1040.94 1041.68	O	$2s^2\,2p^3(^4S)\,4s\ ^3S_1$ $^3S_1$ $^3S_1$	$2p^4\ ^3P_2$ $^3P_1$ $^3P_0$

TABLE I (Continued)

VUV Wavelength of Emitted Radiation, Å	Emitting Species	Upper State	Lower State
1048.22	A	$3p^5\,(^2P)\,4s\,[1/2]_1$	$3p^6\ ^1S_0$
1066.66	A	$3p^5\,(^2P)\,4s\,[3/2]_1$	$3p^6\ ^1S_0$
(1134.17)	N	$2s2p^4\ ^4P_{1/2}$	$2p^3\ ^4S_{3/2}$
(1134.41)		$^4P_{3/2}$	$^4S_{3/2}$
1134.98		$^4P_{5/2}$	$^4S_{3/2}$
1152.15	O	$2s^22p^3(^2D)\,3s\ ^1D_2$	$2p^4\ ^1D_2$
(1163.88)	N	$2p^23d\ ^2D_{5/2}$	$2p^3\ ^2D_{5/2}$
1164.00		$^2D_{5/2}$	$^2D_{3/2}$
1164.21		$^2D_{3/2}$	$^2D_{5/2}$
(1164.32)		$^2D_{3/2}$	$^2D_{3/2}$
1167.45	N	$2p^23d\ ^2F_{7/2}$	$2p^3\ ^2D_{5/2}$
(1168.42)	N	$2p^23d\ ^2F_{5/2}$	$2p^3\ ^2D_{5/2}$
(1168.54)		$3d\ ^2F_{5/2}$	$^2D_{3/2}$
(1176.51)	N	$2p^24s\ ^2P_{3/2}$	$2p^2\ ^2D_{5/2}$
(1176.63)		$^2P_{3/2}$	$^2D_{3/2}$
1177.70		$^2P_{1/2}$	$^2D_{5/2}$
1199.53	N	$2p^23s\ ^4P_{5/2}$	$2p^3\ ^4S_{3/2}$
1200.20		$^4P_{3/2}$	$^4S_{3/2}$
1200.69		$^4P_{1/2}$	$^4S_{3/2}$
(1215.668)	H	$2p\ (^2P_{3/2})$	$1s\ (^2S_{1/2})$
(1215.667)		$2p\ (^2P_{1/2})$	$1s\ (^2S_{1/2})$
1217.64	O	$2s^22p^3(^2P)\,3s\ ^1P_1$	$2p^4\ ^1S_0$
(1225.03)	N	$2p^24d\ ^2D_{5/2}$	$2p^3\ ^2P_{3/2}$
(1225.37)		$4d\ ^2D_{3/2}$	$^2P_{1/2}$
(1228.43)	N	$2p^24d\ ^2P_{1/2}$	$2p^3\ ^2P_{1/2}$
(1228.78)		$4d\ ^2P_{3/2}$	$^2P_{3/2}$

TABLE I (Continued)

VUV Wavelength of Emitted Radiation, Å	Emitting Species	Upper State	Lower State
(1243.18 1243.31)	N	$2p^2\,3s\ {}^2D_{5/2}$ $\quad {}^2D_{3/2}$	$2p^3\ {}^2D_{5/2}$ $\quad {}^2D_{3/2}$
(1277.25 1277.28 1277.51 1277.55 1277.72 1277.95)	C	$2s^2\,2p(^2p)\,3d\ {}^3D_1$ $\quad {}^3D_2$ $\quad {}^3D_1$ $\quad {}^3D_3$ $\quad {}^3D_2$ $\quad {}^3D_1$	$2p^2\ {}^3P_0$ $\quad {}^3P_1$ $\quad {}^3P_1$ $\quad {}^3P_2$ $\quad {}^3P_2$ $\quad {}^3P_2$
1302.17 1304.86 1306.03	O	$2s^2\,2p^3(^4S)\,3s\ {}^3S_1$ $\quad {}^3S_1$ $\quad {}^3S_1$	$2p^4\ {}^3P_2$ $\quad {}^3P_1$ $\quad {}^3P_0$
1310.54 (1310.94 1310.95)	N	$2p^2\,3d\ {}^2D_{5/2}$ $\quad {}^2D_{3/2}$ $\quad {}^2D_{3/2}$	$2p^3\ {}^2P_{3/2}$ $\quad {}^2P_{1/2}$ $\quad {}^2P_{1/2}$
(1318.998 1319.005) (1319.67 1319.68)	N	$2p^2\,3d\ {}^2P_{1/2}$ $\quad {}^2P_{1/2}$ $\quad {}^2P_{3/2}$ $\quad {}^2P_{3/2}$	$2p^3\ {}^2P_{1/2}$ $\quad {}^2P_{3/2}$ $\quad {}^2P_{1/2}$ $\quad {}^2P_{3/2}$
(1326.56 1326.57) (1327.917 1327.924)	N	$2p^2\,4s\ {}^2P_{3/2}$ $\quad {}^2P_{3/2}$ $\quad {}^2P_{1/2}$ $\quad {}^2P_{1/2}$	$2p^3\ {}^2P_{1/2}$ $\quad {}^2P_{3/2}$ $\quad {}^2P_{1/2}$ $\quad {}^2P_{3/2}$
1355.60 1358.51	O	$2s^2\,2p^3\,(^4S)\,3s\ {}^5S_2$ $\quad 3s\ {}^5S_2$	$2p^4\ {}^3P_2$ $\quad {}^3P_1$
1383.97	N_2	$a^1\Pi_g\,(v' = 2)$	$X^1\Sigma_g^+\,(v'' = 0)$
1408.86	CO	$A^1\Pi\ (v' = 6)$	$X^1\Sigma^+\,(v'' = 1)$
(1411.93 1411.94 1411.95)	N	$2p^2\,3s\ {}^2D_{3/2}$ $\quad {}^2D_{3/2}$ $\quad {}^2D_{5/2}$	$2p^3\ {}^2P_{1/2}$ $\quad {}^2P_{3/2}$ $\quad {}^2P_{3/2}$
1416.08	N_2	$a^1\Pi_g\,(v' = 1)$	$X^1\Sigma_g^+\,(v'' = 0)$
1418.91	CO	$A^1\Pi\,(v' = 4)$	$X^1\Sigma^+\,(v'' = 0)$
1447.27	CO	$A^1\Pi\,(v' = 3)$	$X^1\Sigma^+\,(v'' = 0)$

TABLE I (Continued)

VUV Wavelength of Emitted Radiation, Å	Emitting Species	Upper State	Lower State
1450.30	N_2	$a^1\Pi_g (v' = 0)$	$X^1\Sigma_g^+ (v'' = 0)$
1463.34	C	$2s^2\,2p(^2P)\,3d\ ^1F_3$	$2p^2\ ^1D_2$
1463.4	CO	$A^1\Pi (v' = 4)$	$X^1\Sigma^+ (v'' = 1)$
1464.1	N_2	$a^1\Pi_g (v' = 1)$	$X^1\Sigma_g^+ (v'' = 1)$
1477.48	CO	$A^1\Pi (v' = 2)$	$X^1\Sigma^+ (v'' = 0)$
(1492.63 1492.82) 1494.76	N	$2p^2\,3s\ ^2P_{3/2}$ $^2P_{3/2}$ $^2P_{3/2}$	$2p^3\ ^2D_{5/2}$ $^2D_{3/2}$ $^2D_{3/2}$
1500.7	N_2	$a^1\Pi_g (v' = 0)$	$X^1\Sigma_g^+ (v'' = 1)$
1509.66	CO	$A^1\Pi (v' = 1)$	$X^1\Sigma^+ (v'' = 0)$
1515.2	N_2	$a^1\Pi_g (v' = 1)$	$X^1\Sigma_g^+ (v'' = 2)$
1529.9	N_2	$a^1\Pi_g (v' = 2)$	$X^1\Sigma_g^+ (v'' = 3)$
1542.34	CO	$A^1\Pi (v' = 3)$	$X^1\Sigma^+ (v'' = 2)$
1554.73	N_2	$a^1\Pi (v' = 0)$	$X^1\Sigma_g^+ (v'' = 2)$
1559.47	CO	$A^1\Pi (v' = 4)$	$X^1\Sigma^+ (v'' = 3)$
(1560.31 1560.68 1560.71 1561.34 1561.37 1561.44)	C	$2p^3\ ^3D_1$ $^3D_2$ $^3D_1$ $^3D_2$ $^3D_1$ $^3D_3$	$2p^2\ ^3P_0$ $^3P_1$ $^3P_1$ $^3P_2$ $^3P_2$ $^3P_2$
1576.67	CO	$A^1\Pi (v' = 2)$	$X^1\Sigma^+ (v'' = 2)$
1584.4	N_2	$a^1\Pi_g (v' = 2)$	$X^1\Sigma_g^+ (v'' = 4)$
1597.14	CO	$A^1\Pi (v' = 2)$	$X^1\Sigma^+ (v'' = 2)$
1611.26	CO	$A^1\Pi (v' = 4)$	$X^1\Sigma^+ (v'' = 4)$

TABLE I (Concluded)

VUV Wavelength of Emitted Radiation, Å	Emitting Species	Upper State	Lower State
1611.67	N_2	$a^1\Pi_g (v' = 0)$	$X^1\Sigma_g^+ (v'' = 3)$
1626.5	N_2	$a^1\Pi g (v' = 1)$	$X^1\Sigma_g^+ (v'' = 4)$
1630.40	CO	$A^1\Pi (v' = 2)$	$X^1\Sigma^+ (v'' = 3)$
1635.02	CO	$A^1\Pi (v' = 0)$	$X^1\Sigma^+ (v'' = 2)$
1656.27	C	$2s^2\,2p(^2P)\,3s\ ^3P_2$	$2p^2\ ^3P_1$
1656.93		$^3P_1$	$^3P_0$
1657.01		$^3P_2$	$^3P_2$
1657.38		$^3P_1$	$^3P_1$
1657.91		$^3P_1$	$^3P_1$
1658.12		$^3P_1$	$^3P_2$
1669.68	CO	$A^1\Pi (v' = 1)$	$X^1\Sigma^+ (v'' = 3)$
1672.14	N_2	$a^1\Pi_g (v' = 0)$	$X^1\Sigma_g^+ (v'' = 4)$
1687.63	N_2	$a^1\Pi g (v' = 1)$	$X^1\Sigma_g^+ (v'' = 5)$
1712.19	CO	$A^1\Pi (v' = 0)$	$X^1\Sigma^+ (v'' = 3)$
1729.25	CO	$A^1\Pi (v' = 1)$	$X^1\Sigma^+ (v'' = 4)$
1736.2	N_2	$a^1\Pi_g (v' = 0)$	$X^1\Sigma_g^+ (v'' = 5)$
1742.72	N	$2p^2\,3s\ ^2P_{3/2}$	$2p^3\ ^2P_{1/2}$
1742.73		$^2P_{3/2}$	$^2P_{3/2}$
1745.25		$^2P_{1/2}$	$^2P_{1/2}$
1745.26		$^2P_{1/2}$	$^2P_{3/2}$
1751.9	N_2	$a^1\Pi_g (v' = 1)$	$X^1\Sigma_g^+ (v'' = 6)$
1768.1	N_2	$a^1\Pi g (v' = 2)$	$X^1\Sigma_g^+ (v'' = 7)$
1774.90	CO	$A^1\Pi (v' = 0)$	$X^1\Sigma^+ (v'' = 4)$
1792.38	CO	$A^1\Pi (v' = 1)$	$X^1\Sigma^+ (v'' = 5)$
1804.7	N_2	$a^1\Pi_g (v' = 0)$	$X^1\Sigma_g^+ (v'' = 6)$
1810.82	CO	$A^1\Pi (v' = 2)$	$X^1\Sigma^+ (v'' = 6)$
1820.8	N_2	$a^1\Pi_g (v' = 1)$	$X^1\Sigma_g^+ (v'' = 7)$
1837.2	N_2	$a^1\Pi g (v' = 2)$	$X^1\Sigma_g^+ (v'' = 8)$
1859.41	CO	$A^1\Pi (v' = 1)$	$X^1\Sigma^+ (v'' = 6)$
1930.91	C	$2s^2\,2p(^2P)\,3s\ ^1P_1$	$2p^2\ ^1D_2$

TABLE II

DESLANDRES TABLE OF THE OBSERVED N_2 BANDHEADS OF THE LYMAN-BIRGE-HOPFIELD SYSTEM

v' \ v''	0	1	2	3	4	5	6	7
0	68,951.2	66,636	64,320.0	62,047.6	59,803.5	57,597	55,411	
1	70,617.6	68,301	65,998		61,482	59,254.6	57,081	54,921
2	72,256.2			65,364	63,115			56,558

(Wavenumbers, cm^{-1})

TABLE III
DESLANDRES TABLE OF THE OBSERVED CO BANDHEADS OF THE FOURTH POSITIVE SYSTEM

v' \ v''	0	1	2	3	4	5	6
0		62,611.8	60,495.5	58,404.7	56,341.3		
1	66,240.0			59,891.8	57,828.7	55,791.7	53,780.4
2	67,682.9		63,425.0	61,334.6			55,223.8
3	69,095.4		64,836.4				
4	70,476.6	68,333.3		64,124.4	62,063.3		
5							
6		70,979.6					

(Wavenumbers, cm^{-1})

TABLE IV
WAVELENGTHS OF NORMALLY OBSERVED LINE
RADIATION FROM THE ARGON PLASMA

Argon, Å		Nitrogen, Å	Oxygen, Å	Carbonm Å	Hydrogen, Å
(797.75	826.36	(1134.17	1302.17	(1277.25	(1215.667
797.88)	834.39	1134.41)	1304.86	1277.28	1215.668)
798.17	835.00	1134.98	1306.03	1277.51	
	842.81	1199.53	1355.60	1277.55	
(801.36	866.81	1200.20		1277.72	
801.39)	869.75	1200.69		1277.95)	
802.86	876.06			1463.34	
	879.95	(1243.18			
(806.88	894.31	1243.31)		(1560.31	
807.22)	1048.22	(1411.93		1560.68	
809.93	1066.66	1411.94		1560.71	
		1411.95)		1561.34	
(816.23				1561.37	
816.47)		(1492.63		1561.44)	
820.13		1492.82)		(1656.27	
		1494.76		1656.93	
825.35				1657.01	
		(1742.72		1657.38	
		1742.73)		1657.91	
		(1745.25		1658.12)	
		1745.26)		1930.91	

TABLE V
WAVELENGTHS OF NORMALLY OBSERVED LINE
RADIATION FROM THE NITROGEN PLASMA

Nitrogen, Å			Oxygen, Å	Carbon, Å	Hydrogen, Å
1134.17	1225.03	1411.93	1302.17	1560.38	1215.667
1134.41	1225.37	1411.94	1304.86	1560.68	1215.668
1134.98	1228.43	1411.95	1306.03	1560.71	
1163.88	1228.78	1492.63		1561.34	
1164.00	1243.18	1492.82		1561.37	
1164.21	1243.31	1494.77		1561.44	
1164.32	1310.54	1742.72		1656.27	
1167.45	1310.94	1742.73		1656.93	
1168.42	1310.95	1745.25		1657.01	
1168.54	1319.00	1745.26		1657.38	
1176.51	1319.01			1657.91	
1176.63	1319.67			1658.12	
1177.70	1319.68			1930.91	
1199.53	1326.56				
1200.20	1326.57				
1200.69					

DOCUMENT CONTROL DATA - R & D

(Security classification of title, body of abstract and indexing annotation must be entered when the overall report is classified)

1. ORIGINATING ACTIVITY *(Corporate author)*
Arnold Engineering Development Center
ARO, Inc., Operating Contractor
Arnold Air Force Station, Tennessee

2a. REPORT SECURITY CLASSIFICATION
UNCLASSIFIED

2b. GROUP
N/A

3. REPORT TITLE
VACUUM ULTRAVIOLET RADIATION EMITTED FROM ARC-JET PLASMAS OF ARGON OR NITROGEN

4. DESCRIPTIVE NOTES *(Type of report and inclusive dates)*
August 1, 1967 - August 1, 1968 - Final Report

5. AUTHOR(S) *(First name, middle initial, last name)*
G. E. Staats and W. K. McGregor, Jr., ARO, Inc. and A. A. Mason, The University of Tennessee Space Institute

6. REPORT DATE
October 1968

7a. TOTAL NO. OF PAGES
50

7b. NO. OF REFS
15

8a. CONTRACT OR GRANT NO.
F40600-69-C-0001

b. PROJECT NO. 8951

c. Program Element 61102F

d. Task 895105

9a. ORIGINATOR'S REPORT NUMBER(S)
AEDC-TR-68-171

9b. OTHER REPORT NO(S) *(Any other numbers that may be assigned this report)*
N/A

10. DISTRIBUTION STATEMENT
This document has been approved for public release and sale; its distribution is unlimited.

11. SUPPLEMENTARY NOTES
Available in DDC

12. SPONSORING MILITARY ACTIVITY
Arnold Engineering Development Center, Air Force Systems Command, Arnold Air Force Station, Tennessee

13. ABSTRACT
Vacuum ultraviolet emission in the range from 2000 to 700 Å was observed for both argon and nitrogen plasmas, produced by a Gerdien-type arc-jet freely expanding into a vacuum cell. The experimental setup centers about a simple, one-meter, concave grating spectrograph mounted within a tank purged with helium. Other gases were allowed to mix with the flowing plasma so that the physical mechanisms of excitation within the plasma could be studied. Over 50 atomic lines and three band systems were identified in mapping the spectral region. Mechanisms to produce the radiation observed are postulated, and some unexplained phenomena are also discussed.

14 KEY WORDS	LINK A		LINK B		LINK C	
	ROLE	WT	ROLE	WT	ROLE	WT
plasma radiation						
argon						
~~nitrogen~~						
~~ultraviolet spectra~~						
vacuum spectroscopy						
~~plasma jets~~						

1. Plasmas -- Radiation
2 Argon plasmas
3 Nitrogen "

15-20.